Location of Fluoride Counterion in As-Synthesized Silicalite-1 by Single Crystal X-Ray Diffraction

ARTICLE *in* THE JOURNAL OF PHYSICAL CHEMISTRY B · FEBRUARY 2002

Impact Factor: 3.3 · DOI: 10.1021/jp012231d

5 AUTHORS, INCLUDING:

Emmanuel Aubert
University of Lorraine
67 PUBLICATIONS **430** CITATIONS
SEE PROFILE

Florence Porcher
Atomic Energy and Alternative Energies Com…
102 PUBLICATIONS **746** CITATIONS
SEE PROFILE

Mohamed Souhassou
French National Centre for Scientific Research
99 PUBLICATIONS **1,495** CITATIONS
SEE PROFILE

Location of Fluoride Counterion in As-Synthesized Silicalite-1 by Single Crystal X-ray Diffraction†

Emmanuel Aubert,‡ Florence Porcher,‡ Mohamed Souhassou,‡ Václav Petříček,§ and Claude Lecomte*,‡

Laboratoire de Cristallographie et Modélisation des Matériaux Minéraux et Biologiques, UMR CNRS No. 7036, Université Henri Poincaré Nancy 1, Faculté des Sciences, BP 239, 54506 Vandœuvre-lès-Nancy Cedex, France, and Institute of Physics, Academy of Sciences of the Czech Republic, Na Slovance 2, 182 21 Praha 8, Czech Republic

Received: June 13, 2001; In Final Form: October 10, 2001

This paper presents results from single-crystal X-ray diffraction at room temperature on as-synthesized tetrapropylammonium fluoride silicalite. The fluoride counteranion lies in a $[4^15^26^2]$ cage on a general position at an interacting distance from a silicon framework atom (Si−F = 1.915(3) Å). This silicon atom is close to the center of a slightly distorted trigonal bypyramid consisting of four oxygen framework atoms and a fluoride anion. The Si−O apical bond distance (1.667(2) Å) is clearly longer than the Si−O basal bond distances (1.62 ± 0.01 Å). The occluded TPA^+ cation is described using a disordered model at the channels intersection.

Introduction

Zeolites (or more generally microporous materials) are commonly used as supports for adsorption of small organic molecules and understanding of the interactions involved in these phenomena may provide information about chemical selectivity of these materials and physical properties of the host molecules.

MFI (Mobil-five) materials exhibit a network of straight and sinusoidal channels with free apertures of approximately 5.4 × 5.6 and 5.1 × 5.4 Å respectively,[1] both built by 10-membered ring openings (Figure 1). These channels are respectively along the [010] and [100] directions in the case of orthorhombic MFI materials.

High-resolution X-ray single crystal diffraction is one of the best tools for studying zeolite−guest interactions, but it requires large enough single crystals of high crystal quality. Silicalite, the all-silica end member of MFI type materials, is one of the rare microporous materials that can be grown as large crystals (300 μm). Most of the syntheses involve the use of a structure directing agent (SDA) (in general, the tetrapropylammonium cation TPA^+). Crystallization can be done in high pH hydroxide media or in neutral/slightly acidic media in which the solubility of silica species is ensured by fluoride. From these two routes, the counteranions associated with TPA^+ are respectively OH^- and F^-. The crystals obtained without subsequent treatments are called "as-synthesized". Although there have been a few studies dealing with structural investigation of as-synthesized MFI materials using different techniques, the symmetry, the location of the SDA and of its counteranion are not clear.

While in this publication we are interested in the study of silicalite (purely siliceous MFI materials), lot of works have been devoted to MFI materials containing aluminum in substitution of silicon framework atoms (see references below). It should be kept in mind that such substitutions (or more generally substitutions with other T atoms, T = Fe, ...) introduce charges on the framework that must be taken into account for the charge compensation process. Moreover, substitution of silicon atoms in the framework could be associated also with framework defects (see below).

Crystal Symmetry. *Pnma* is the commonly accepted space group for as-synthesized MFI zeolites, as checked by powder[2] and single-crystal X-ray diffraction.[3] This has been more recently assessed by Fyfe et al.[4] who observed twelve individual peaks in the high resolution $^1H \rightarrow {}^{29}Si$ cross polarization (CP) MAS spectrum (at 327 K). These twelve peaks correspond to the twelve independent silicon sites required to describe the structure using space group *Pnma*. However, Price et al.[5] reported an oblique extinction (0.3°) in MFI crystals observed by optical microscopy, which may indicate a monoclinic symmetry that differs from an orthorhombic symmetry by less than 0.1°.

Extraframework Species: TPA^+ Cation. There are many discrepancies about the location of TPA^+ among published results. First, not all structural studies report the location of this ion. Olson et al.[1] modeled two extraframework entities by oxygen atoms with partial occupancies inside the channels. Other studies proposed a complete model for the TPA^+ at the intersection of the channels, but with different geometric configurations: Baerlocher[6] proposed a unique cation with mirror symmetry in which two propyl arms lie on the mirror and the other two are mirror images. Koningsveld et al.[3] modeled the TPA^+ at the same channel intersection but used two differently populated orientations approximately related by a pseudomirror (local symmetry). This latter study also reported previous literature results and compares the configurations found for the TPA^+: the main differences are due to the models used (disordered or not), to the symmetry of the cation, and to the geometrical parameters.

Extraframework Species: Counteranion. In their studies by X-ray diffraction of as-synthesized MFI crystals grown in

† This paper is specially dedicated to Pr. Yves Dusausoy, who initiated the studies of zeolites at the LCM³B, on the occasion of his retirement.

* Corresponding author. E-mail: lecomte@lcm3b.uhp-nancy.fr. Fax number: (33) 3-83-40-64-92.

‡ Université Henri Poincaré Nancy 1.

§ Academy of Sciences of the Czech Republic.

10.1021/jp012231d CCC: $22.00
Published on Web 01/09/2002

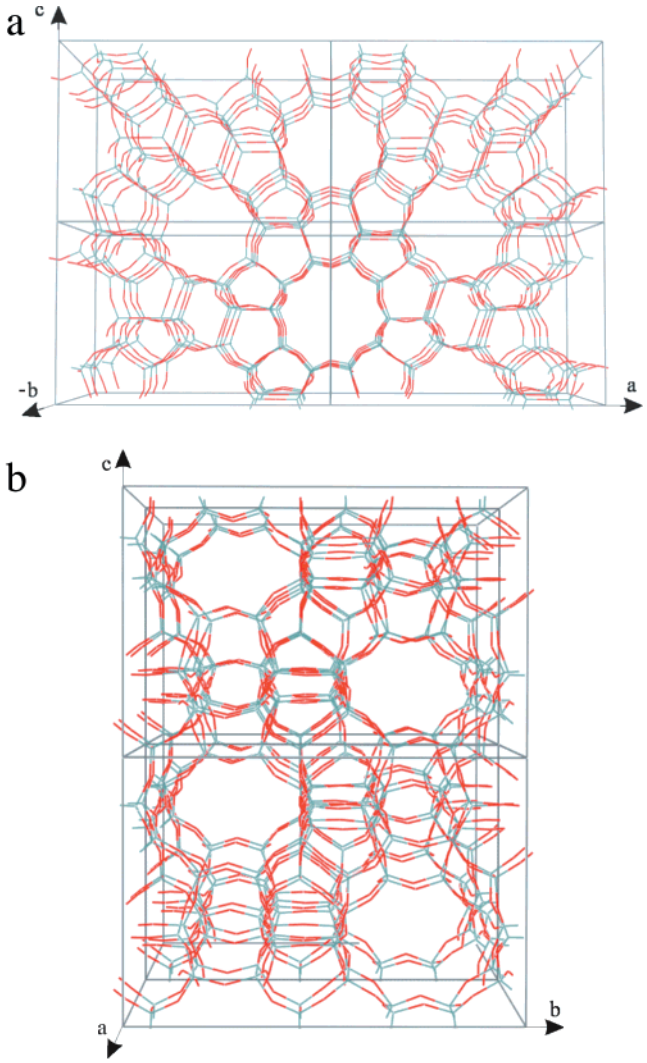

Figure 1. (a) View along the [010] direction (straight channels). (b) View along the [100] direction (sinusoidal channels). Oxygen atoms in red and silicon atoms in gray.

hydroxide media, Baerlocher[6] and Koningsveld et al.[3] did not report the location of the OH^- anions. For crystals grown in fluoride media, Price et al.[5] found the F^- anion close to the carbon atoms (C−F distance of 2.11(9) Å) of the TPA^+ at the channels intersection and on the *Pnma* mirror *m*. This disagrees with the powder diffraction results of Mentzen et al.[7] who found F^- far away from the TPA^+ molecule on the *m* mirror in a $[4^15^26^2]$ cage[8] with a Si−F distance of 2.20(4) Å. The latter study also proposed another unassigned extraframework peak close to the TPA^+. Using NMR techniques, Koller et al.[9,10] showed that the fluoride anion interacts with silicon atoms, leading to $SiO_{4/2}F^-$ units. More recently Fyfe et al.[4] determined the Si−F distances by multinuclear NMR spectroscopy, from which they calculated the fractional coordinates of F^- using the structural framework proposed by Koningsveld et al.[3]: the fluoride anion lies inside the $[4^15^26^2]$ cage on the *m* mirror in a site similar to that proposed by Mentzen et al.[7]

For several years our group has been involved in accurate crystal structure determinations in zeolites in order to calculate electrostatic properties.[11−13] The present study is devoted to structural investigation of an as-synthesized fluoride silicalite using single crystal X-ray diffraction to accurately locate the F^- anion and provide an occupancy model for the occluded TPA^+ cation. Such a study may aid understanding of the crystallization processes (role of SDA, template) and of interactions between zeolites and guest molecules.

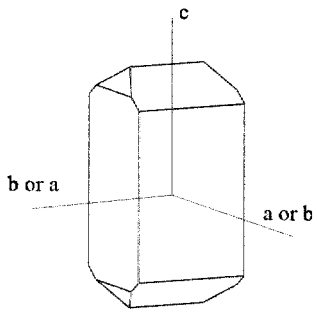

Figure 2. Morphology of the MFI crystal studied.

Experimental Section

Synthesis. The crystal used in our experiment was grown according to the fluoride route proposed by Guth et al.[14] This fluoride route allows the crystallization of large crystals of aluminum-free MFI materials containing few defects in comparison to other synthesis methods (a description of the nature and number of such defects is given by Chézeau et al.[20] using NMR spectroscopy).[4,21] The molar composition of the initial gel was 1 SiO_2:0.12 NH_4HF_2:0.14 TPABr:38.81 H_2O. Reactors were placed in a preheated oven at 453 K for 20 days. Then the reactors were quenched and cooled with cold water, and the reaction products were filtered, washed with water, and dried overnight at approximately 353 K in an oven.

Optical microscopy showed that all products were MFI crystals with a morphology similar to that described by Guth et al.[14] (Figure 2). All crystals presented a hourglass pattern when examined between cross polarizers, indicating a possible twinning (Weidenthaler et al.[15]). SEM photographs were taken, and semiquantitative chemical analyses did not show the presence of aluminum. As silicalite crystals synthesized in fluoride medium are known to be highly hydrophobic, no special care (capillary) was taken to prevent them from exposition to moisture. For the following, the chemical composition of the as-synthesized crystals was assumed to be $Si_{96}O_{192}$:4($NC_{12}H_{28}$):4F.

X-ray Data Collection and Processing. The X-ray diffraction experiment was carried out at room temperature using an Enraf Nonius Kappa CCD diffractometer with monochromatized Mo(Kα) radiation on a 330 μm × 140 μm × 140 μm crystal (Figure 2). Diffraction frames collected by the oscillating crystal method were processed using program HKL2000.[16] Reflection intensities were integrated using a pseudotetragonal orthorhombic cell that refined to $a = 20.0026(2)$ Å, $b = 19.9934(2)$ Å, $c = 13.3923(1)$ Å. No absorption correction was applied ($\mu = 6.9$ cm^{-1}). Reflection intensities were averaged[17] in point group *mmm* with an internal agreement factor $R^i = 0.059$ for all reflections. The experimental conditions are summarized in Table 1.

Careful investigation of reflection intensities showed the *n* glide plane systematic extinctions plus unusual extinction conditions: for reflections *h*00, 0*k*0, 00*l*: *h*, *k*, $l = 2n + 1$ and for *hk*0: *h and k* $= 2n + 1$. This latter condition is satisfied by considering that the specimen studied is twinned, composed of *Pnma* or $Pn2_1a$ domains related by a 2-fold twin axis along the [110] direction. These observations confirmed the twinning of the crystal, as expected from the optical microscope examination. Because the *a* and *b* cell parameters of monocrystalline high-silica MFI materials are very similar (Koningsveld et al.[3]),

TABLE 1: Experimental Conditions

compound	$Si_{96}O_{192}$:4($NC_{12}H_{28}$):4F
space group	*Pnma*, crystal twinned, twin operator [110]2
size	330 μm × 140 μm × 140 μm
temperature	room temperature
diffractometer	ENRAF NONIUS Kappa CCD
X-ray source	sealed tube Mo(Kα)
wavelength	$\lambda = 0.7107$ Å
absorption coefficient	$\mu = 6.9$ cm^{-1}
oscillation width	2°/frame
exposure time	90 s/°
cell parameters	$a = 20.0026(2)$ Å
	$b = 19.9934(2)$ Å
	$c = 13.3923(1)$ Å
$(\sin\theta/\lambda)_{max}$	1.02 Å^{-1}
no. of reflns measured	77 896
no. of unique reflns	43 831
no . of unique obsd reflns ($I > 3s(I)$)	20 965
$R^i = \Sigma\|I - \langle I\rangle\|/\Sigma\|I\|$	
all reflns	0.059
reflns with sin $\theta/\lambda < 0.71$ Å^{-1} and $I/\sigma(I) > 3$	0.036
$R^i_w = (\Sigma w(I - \langle I\rangle)^2/\Sigma wI^2)^{1/2}$ with $w = 1/\sigma(I)^2$	
all reflns	0.054
reflns with sin $\theta/\lambda < 0.71$ Å^{-1} and $I/\sigma(I) > 3$	0.047

the diffracted spots *hkl* (domain 1) and *khl* (domain 2) totally overlap on CCD frames and cannot be integrated separately. The unit cell parameters used afterward (in particular for the calculation of distances) are those refined from the studied twinned crystal. The choice of the *Pnma* space group was confirmed by the success of the refinement (see below).

Structure Refinement. The structure refinements (including refinement of the twin parameter) were performed with the program Jana2000 (Petříček and Dušek[18]). In this program, the squares of the structure factor moduli of a twinned crystal are expressed as the weighted sum of the squares of the structure factor moduli of each "single" domain, which lead in our case to $F^2(hkl) = \upsilon_1 F^2(hkl) + \upsilon_2 F^2(khl)$ (υ_1 and υ_2 are the volume fraction of domains 1 and 2 related by the twin operator). The search for non-modeled atoms to complete the structure by difference Fourier maps requires a definition of an "observed" structure factor related to only one domain. In our case, we used the fraction correction option ($F_{obs,1} = F_{obs}(F_{calc,1}/F_{calc})$, where $F_{obs,1}$ and $F_{calc,1}$ are respectively observed and calculated structure factors from the first domain and F_{calc} is the calculated structure factor of the twin calculated as mentioned above[18]).

The form factors used for the refinements were those of neutral free atoms.[19] The refinement was performed with reflections having sin $\theta/\lambda < 0.71$ Å^{-1}, as the signal-to-noise ratio was too poor at higher resolution. The structure modeling was started using fractional coordinates (x, y, z) and isotropic atomic displacement parameters (U_{iso}) of the framework of a silica rich zeolite ZSM-5 (Koningsveld et al.[3]). After refinement of x, y, z, U_{iso}, scale factor, and twin parameter [0.481(2)], the agreement factors dropped to $R = 0.104$, $Rw = 0.163$, and Gof = 8.56 (Table 2).

The first residual peak in difference Fourier maps ($\rho = 5.2$ e Å^{-3}) was located in a small [$4^1 5^2 6^2$] cage ~0.5 Å away from the mirror [010]m, at approximately 1.9 Å from Si9. The next two peaks ($\rho = 4.2$ and 2.8 e Å^{-3}) lie in the channels. The first peak was modeled as a fluorine atom labeled Fx. Refinement of its fractional coordinates, isotropic atomic displacement parameters (ADP), and occupancy dropped the R, Rw, and Gof factors respectively to 0.094, 0.145 and 7.61. The second and third peaks were modeled as nitrogen and carbon atoms belonging to disordered TPA^+ cations. Subsequent refinement cycles and difference Fourier maps revealed a total of eighteen carbon atoms of TPA^+ inside the channels. All these carbon atoms were introduced using partial occupancy factors chosen according to the site symmetry of the TPA atoms; the partial occupancies were kept fixed considering the disorder and the twinning of the structure.

After refinement of all structural parameters (isotropic ADP for carbon atoms, occupancy and anisotropic ADP for Fx), there were important discrepancies among the N−C and C−C distances (C−C = 1.29 Å, for example). Distance restraints were then introduced for nitrogen−carbon and carbon−carbon bonds (1.51 ± 0.02 Å) in order to improve the chemical reliability of the model of TPA^+. These restraints required the assignment of propyl arms to disordered TPA^+ cations. This was not straightforward because of the proximity of fractional carbon atoms that could be reasonably assigned to disordered propyl groups. These ambiguities in the choice of a restrained configuration were resolved by assuming that the best starting configuration was that offering the best C−C distances regardless of the C−C−C or N−C−C bond angles. Indeed, interactions between TPA^+ and the zeolite framework can distort bond angles but have much smaller effects on bond distances. This defines *one* model for the propyl chains; however, it should be noted that this model is not unique. With this definition of the propyl arms, the refinement converged to $R = 0.034$, $Rw = 0.048$, Gof = 2.57 (compared to $R = 0.034$, $Rw = 0.048$, Gof = 2.55 for the unrestrained model of TPA^+); the twin parameter refined to 0.4770(9). Final parameters are summarized in Table 3. In the last cycle the maximum shift/esd was −0.017 for fractional coordinate x of atom C7b and the deepest hole (−0.45 e Å^{-3}) was at 0.23 Å from O13. The main residual peaks were located very close to the atoms (0.63 e Å^{-3} at 0.35 Å from O13, 0.62 e Å^{-3} at 0.58 Å from C1a) and, as expected, cannot be attributed to localized water molecules.

Another refinement of the crystal structure with split Si9 position was also attempted in order to model the disorder suggested by the elongated atomic displacement ellipsoid. It

TABLE 2: Refinements Characteristics[a]

refinement description	framework Si,O	framework Si,O + Fx	framework Si,O + Fx,N,C	framework Si,O + Fx,N,C TPA N−C C−C bonds restrained
$(\sin\theta/\lambda)_{max}$, Å^{-1}	0.71	0.71	0.71	0.71
no. of reflns used ($I > 3\sigma(I)$)	7634	7634	7634	7634
no. of params	150	155	413	413
R	0.104	0.094	0.034	0.034
wR_F	0.163	0.145	0.048	0.048
GoF	8.56	7.61	2.55	2.57
twin param	0.481(2)	0.480(2)	0.4770(9)	0.4770(9)

[a] $R = (\Sigma||F_{obs}| - |F_{calc}||)/(\Sigma|F_{obs}|)$. $wR_F = ((\Sigma w'(|F_{obs}| - |F_{calc}|)^2)/(\Sigma w'|F_{obs}|^2))^{1/2}$. Gof = $((\Sigma w(|F_{obs}| - |F_{calc}|)^2)/(m - n))^{1/2}$. F_{obs} and F_{calc} are the observed and calculated structure factors scaled one to the other, respectively. $w = 1/\sigma(F_{obs})^2$, $w' = w/(4F_{obs}^2)$, m is the number of reflections, and n is the number of refined parameters. R factors are calculated over observed reflections ($I > 3\sigma(I)$).

TABLE 3: Atomic Fractional Coordinates and Equivalent Displacement Parameters (Same Labeling as Koningsveld et al.[3]) for Si, O[a]

label	*x*	*y*	*z*	U_{eq} (Å^2)	occupancy	multiplicity
Si1	0.42481(3)	0.05838(3)	−0.33946(5)	0.0128(2)	1	8
Si2	0.30953(3)	0.03079(4)	−0.19505(5)	0.0128(2)	1	8
Si3	0.28126(4)	0.06160(3)	0.02796(5)	0.0128(2)	1	8
Si4	0.12333(4)	0.06311(3)	0.02602(5)	0.0121(2)	1	8
Si5	0.07328(4)	0.02692(4)	−0.18775(5)	0.0132(2)	1	8
Si6	0.18631(4)	0.06131(4)	−0.33284(5)	0.0159(2)	1	8
Si7	0.42379(3)	−0.17249(3)	−0.32668(5)	0.0116(2)	1	8
Si8	0.30885(4)	−0.12731(3)	−0.18739(5)	0.0134(2)	1	8
Si9	0.26972(4)	−0.17583(4)	0.02593(6)	0.0203(3)	1	8
Si10	0.11878(4)	−0.17382(3)	0.02954(5)	0.0149(2)	1	8
Si11	0.07208(4)	−0.13127(3)	−0.18527(5)	0.0130(2)	1	8
Si12	0.18789(4)	−0.17288(3)	−0.32242(5)	0.0121(2)	1	8
O1	0.3723(1)	0.0637(1)	−0.2494(2)	0.0300(7)	1	8
O2	0.3097(1)	0.0585(1)	−0.0831(2)	0.0280(6)	1	8
O3	0.2020(1)	0.0597(2)	0.0273(2)	0.0454(8)	1	8
O4	0.0973(1)	0.0615(1)	−0.0858(2)	0.0286(7)	1	8
O5	0.1145(1)	0.0566(1)	−0.2792(2)	0.0248(6)	1	8
O6	0.2424(1)	0.0538(1)	−0.2482(2)	0.0373(8)	1	8
O7	0.3732(1)	−0.1617(1)	−0.2369(2)	0.0286(6)	1	8
O8	0.3055(1)	−0.1473(1)	−0.0731(2)	0.0262(6)	1	8
O9	0.1944(1)	−0.1495(1)	0.0463(2)	0.0251(6)	1	8
O10	0.0929(1)	−0.1639(1)	−0.0824(2)	0.0358(7)	1	8
O11	0.1158(1)	−0.1615(1)	−0.2746(2)	0.0251(6)	1	8
O12	0.2435(1)	−0.1487(2)	−0.2474(2)	0.0364(7)	1	8
O13	0.3171(2)	−0.0479(1)	−0.1975(2)	0.0482(9)	1	8
O14	0.0835(1)	−0.0519(1)	−0.1794(2)	0.0341(7)	1	8
O15	0.4275(1)	0.1281(1)	−0.3980(2)	0.0251(6)	1	8
O16	0.4059(1)	−0.0006(1)	−0.4141(2)	0.0345(7)	1	8
O17	0.4003(1)	−0.1316(1)	−0.4236(2)	0.0268(7)	1	8
O18	0.1900(1)	0.1311(1)	−0.3880(2)	0.0212(6)	1	8
O19	0.1913(1)	−0.0001(1)	−0.4098(2)	0.0343(7)	1	8
O20	0.1937(1)	−0.1306(1)	−0.4247(2)	0.0266(7)	1	8
O21	0.0036(1)	0.0445(1)	−0.2080(2)	0.0245(6)	1	8
O22	0.0043(1)	−0.1468(1)	−0.2098(2)	0.0249(6)	1	8
O23	0.4267(2)	−0.25	−0.3562(2)	0.0248(8)	1	4
O24	0.1962(2)	−0.25	−0.3514(2)	0.0309(9)	1	4
O25	0.2912(2)	−0.25	0.0632(2)	0.0173(7)	1	4
O26	0.1065(2)	−0.25	0.0642(2)	0.0184(8)	1	4
Fx	0.7799(2)	0.2254(2)	0.0715(2)	0.023(1)	0.477(6)	8
N	0.5112(3)	0.75	0.1136(3)	0.052(2)	1	4
C1a	0.587(1)	0.75	0.103(2)	0.141(8)	0.5	4
C2a	0.632(1)	0.781(1)	0.170(2)	0.069(5)	0.25	8
C3a	0.699(1)	0.75	0.192(2)	0.097(8)	0.5	4
C4a	0.952(1)	0.775(1)	0.312(1)	0.049(4)	0.25	8
C5a	0.947(1)	0.775(1)	0.224(1)	0.058(5)	0.25	8
C6a	0.885(1)	0.762(2)	0.159(2)	0.086(7)	0.25	8
C7a	0.484(1)	0.685(1)	0.077(1)	0.106(5)	0.5	8
C8a	0.492(1)	0.661(1)	−0.029(1)	0.126(5)	0.5	8
C9a	0.500(1)	0.588(1)	−0.043(1)	0.060(3)	0.5	8
C1b	0.576(1)	0.75	0.176(1)	0.072(4)	0.5	4
C2b	0.638(1)	0.75	0.117(2)	0.107(6)	0.5	4
C3b	0.707(1)	0.75	0.160(2)	0.096(8)	0.5	4
C4b	0.995(1)	0.75	0.273(1)	0.104(6)	0.5	4
C5b	0.923(1)	0.741(3)	0.247(2)	0.092(9)	0.25	8
C6b	0.913(1)	0.75	0.133(2)	0.078(5)	0.5	4
C7b	0.501(1)	0.696(1)	0.033(2)	0.129(6)	0.5	8
C8b	0.508(1)	0.623(1)	0.048(1)	0.081(3)	0.5	8
C9b	0.471(1)	0.588(1)	−0.036(1)	0.067(3)	0.5	8

[a] Note: $U_{eq} = {}^1/_3 \times \mathrm{Trace}(U^{ij})$. U^{ij} is defined as $T(\mathrm{H}) = \exp(-2\pi^2\Sigma_{ij}h_ih_ja_i^*a_j^*U^{ij})$. For carbon atoms U_{iso} is used. Esd's on last digit are indicated between brackets for refined parameters.

resulted in abnormal Si9−O distances (1.567−1.813 Å) with no significant improvement of the residual factors ($R = 0.034$, $Rw = 0.048$, and Gof = 2.59) and was discarded.

TPA$^+$ Modeling. *Propyl Groups.* The propyl groups are labeled C1a−C2a−C3a, C1b−C2b−C3b, C4a−C5a−C6a, C4b−C5b−C6b, C7a−C8a−C9a, and C7b−C8b−C9b (Figure 5a). Table 4 lists N−C and C−C bond distances and N−C−C and C−C−C bond angles obtained at the end of the restrained refinement. There are ambiguities to assign a given carbon atom to one propyl arm. For instance, the C8a−C9a bond length is 1.48 Å and C8b−C9b is 1.52 Å but another assignment for propyl arms (C8a−C9b, C8b−C9a) would give distances of 1.54 Å and 1.40 Å respectively.

TABLE 4: Geometry of TPA and TPA′ [a]

Interatomic TPA Distances (Å) (Restrained during the Refinement)			
N−C1a	1.52(2)	C2b−C3b	1.50(3)
N−C1b	1.54(2)	C4a−C5a	1.56(2)
N−C4a	1.63(2)	C5a−C6a	1.55(3)
N−C4b	1.56(2)	C4b−C5b	1.48(3)
N−C7a	1.49(2)	C5b−C6b	1.55(3)
N−C7b	1.55(2)	C7a−C8a	1.51(2)
C1a−C2a	1.41(3)	C8a−C9a	1.48(2)
C2a−C3a	1.51(3)	C7b−C8b	1.48(2)
C1b−C2b	1.46(3)	C8b−C9b	1.52(2)

N−C−C and C−C−C Bond Angles (deg) in Propyl Groups			
N−C1a−C2a	124(2)	N−C1b−C2b	115(2)
C1a−C2a−C3a	121(2)	C1b−C2b−C3b	125(2)
N−C4a−C5a	108(1)	N−C4b−C5b	116(2)
C4a−C5a−C6a	112(2)	C4b−C5b−C6b	110(2)
N−C7a−C8a	123(1)	N−C7b−C8b	126(2)
C7a−C8a−C9a	117(2)	C7b−C8b−C9b	108(1)

C−N−C Bond Angles (deg) for TPA and TPA′

TPA		TPA′	
C1a−N−C7a	109.6(7)	C1b−N−C7b	119.6(7)
C7a−N−*m*(C7a)	121.1(8)	*m*(C7a)−N−C7b	109.3(8)
m(C7a)−N−C1a	109.6(7)	*m*(C7a)−N−C1b	119.1(6)
C4b−N−C1a	108(2)	C4a−N−C1b	106.5(7)
C4b−N−C7a	104.0(6)	C4a−N−C7b	96.3(8)
C4b−N−*m*(C7a)	104.0(6)	C4a−N−*m*(C7a)	101.7(7)

distortion coefficient TPA: 14.2° distortion coefficient TPA′: 20.9°
total distortion coefficient: $d = 35.1°$

Torsion Angles (deg) around the Nitrogen Atom of the TPA$^+$ Cation

TPA		TPA′	
C7a−N−C4b−C5b*	56/72.5	C7a−N−C7b−C8b	166.6
C8a−C7a−N−C4b	176.2	C8a−C7a−N−C7b	40.6
C7a−N−C1a−C2a*	79.9/145.0	C7a−N−C4a−C5a	64.3
C8a−C7a−N−C1a	61.2	C8a−C7a−N−C4a	141.6
C7a−N−C7a−C8a	67.8	C7a−N−C1b−C2b	85.0
C1a−N−C4b−C5b*	172.3/172.3	C8b−C7a−N−C1b	101.9
C2a*−C1a−N−C4b	32.5/32.5	C7b−N−C4a−C5a	175.6
		C8b−C7b−N−C4a	61.9
		C7b−N−C1b−C2b	53.7

[a] When two values are given they correspond to disorder around *m* for one C atom considered (*).

Conformations of TPA$^+$. Assembly of the disordered propyl fragments to build a TPA$^+$ is also not straightforward. Indeed, we found nine different fractional carbon atoms, including those obtained by mirror symmetry, at bonding distance from the nitrogen atom. To choose among them, we generated all possible combinations of four propyl arms to build a TPA molecule, given the hypothesis that only two crystallographically independent TPA$^+$ (TPA and TPA′) are necessary to describe the nine first carbon atoms. We also assumed that one TPA$^+$ and its mirror image may exist in the channels since TPA$^+$ does not necessary have a *m* symmetry. The selection criterion was based on the hypothesis that the four carbon atoms linked to the nitrogen atom of the ammonium lead to a tetrahedron that is "as regular as possible". This hypothesis does not preclude any distortion of the propyls arms but prevents unreasonable C−N−C angles. For each configuration considered, a distortion coefficient *d* from the perfect tetrahedral geometry was calculated as

$$d = \Sigma_{\mathrm{TPA,TPA'}}(\Sigma_{i=1,6}(\alpha_i - 109.47)^2)^{1/2}$$

where the first sum is over the two TPA$^+$ tetrahedra, and the

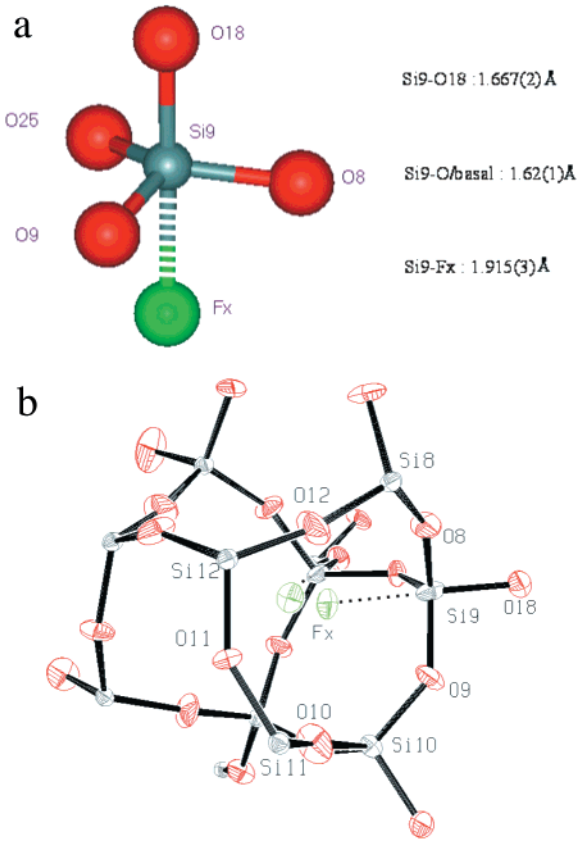

Figure 3. (a) Coordination polyhedron of the Si9 atom. (b) Ortep[34] view of the $[4^15^26^2]$ cage (50% probability ellipsoid).

TABLE 5

Range of Si−O Distances (Å) and O−Si−O Angles (deg)		
Si1	1.591(2)−1.603(2)	107.5(1)−111.5(2)
Si2	1.580(2)−1.598(2)	106.5(1)−111.4(2)
Si3	1.583(2)−1.602(2)	106.8(1)−110.5(2)
Si4	1.575(2)−1.598(2)	108.6(1)−110.5(1)
Si5	1.591(2)−1.603(2)	106.6(1)−110.9(1)
Si6	1.581(2)−1.609(2)	107.3(1)−112.4(1)
Si7	1.587(2)−1.604(2)	107.3(1)−110.9(1)
Si8	1.583(2)−1.603(2)	107.9(2)−112.7(1)
Si9	1.613(2)−1.667(2)	98.6(1)−119.5(2)
Si10	1.598(2)−1.623(2)	105.9(2)−113.5(1)
Si11	1.581(2)−1.605(2)	107.2(1)−110.7(1)
Si12	1.576(2)−1.613(2)	107.0(2)−112.2(2)

Selected Si−O−Si angles (deg)		
angles	Koningsveld et al.[3]	this study
Si9−O9−Si10	154.4	139.1(2)
Si1−O15−Si10	148.2	139.9(2)
Si9−O25−Si9	148.2	132.1(2)
Si2−O13−Si8	175.9	167.1(2)

second sum is over the six C−N−C angles α_i defined for each TPA^+. The configurations obtained have distortion coefficients of (in increasing order) 35.1°, 45.6°, 48.0°, 58.1°, 58.5°, ... The lowest distortion (35.1°) is associated with the following TPA, TPA′ configurations, respectively, formed by C1a, C7a, C4b, *m*(C7a) atoms and C1b, C7b, *m*(C4a), *m*(C7a) atoms (see Figure 5a for the labeling; *m*(atom name) indicates the mirror image of the given atom). Table 4 lists bond angles of these TPA^+.

Framework and Fluorine Atom. The range of Si−O bond distances and O−Si−O bond angles in the framework are summarized in Table 5. All SiO_4 units have quasi tetrahedral geometry, except the Si9 silicon atom, which shows an abnormally long Si−O bond length [1.667(2) Å] as well as a wide range of O−Si−O angles [98.6(1)° to 119.5(2)°]. This

TABLE 6: Stereochemical Parameters of $SiO_{4/2}F^-$ Units[a]

Coordination of Si9 Atom			
Interatomic Distances (Å)			
Si9−O9	1.619(2)	Si9−O18	1.667(2)
Si9−O8	1.613(2)	Si9−Fx	1.915(3)
Si9−O25	1.623(2)		
Interatomic Angles (deg)			
O8−Si9−O9	115.9(1)	O9−Si9−Fx	78.5(1)
O8−Si9−O25	117.3(2)	O25−Si9−Fx	82.8(2)
O9−Si9−O25	119.5(2)	O8−Si9−Fx	81.6(2)
O9−Si9−O18	99.2(2)		
O8−Si9−O18	99.4(1)	O18−Si9−Fx	177.7(2)
O25−Si9−O18	98.6(1)		
Coordination of Fx (Å) Anion			
Fx−Si9	1.915(3)	Fx′−Si9	2.567(3)
Fx−O9	2.247(4)	Fx−Si10	2.646(3)
Fx−O8	2.316(4)	Fx−Si8	3.067(3)
Fx−O25	2.350(4)	Fx′−Si10	3.162(3)

[a] Fx (x, y, x); Fx′(x, $^1/_2 - y$, z).

geometry can be explained by the coordination of the fluoride ion Fx located in a general position in the $[4^15^26^2]$ cage, at 1.915(3) Å from Si9. In fact, Fx forces Si9 to lie close to the center of a slightly distorted trigonal bipyramid (Figure 3a and Table 6) in which O8, O9, and O25 form the basal plane, and Fx and O18 are in the apical positions. The Si9 atom is slightly out of the basal plane [by 0.255(1) Å toward O18] and the distance from Si9 to the apical O18 atom [1.667(2) Å] is longer than the distances to the basal oxygen atoms [1.619(2) Å, 1.623(2) Å, 1.613(2) Å]. Evidently, the presence of the fluoride anion weakens the O18−Si9 bond.

Discussion

Static/Dynamic Model of the Structure. If we consider that a diffraction experiment lasts for several days, the "time scale" for a single crystal X-ray diffraction experiment is of the order of a few days. Therefore, this technique can only provide an "image" of the structure averaged on space (crystal size) and time (duration of the experiment). Thus, we only discuss averaged models for fluoride anion and TPA cations whose nature (static or dynamic) cannot be assessed by a unique diffraction experiment (unique temperature experiment). The NMR technique, whose time scale is considerably shorter, is more suitable to probe dynamical behavior of occluded moieties in zeolites.[22,23]

Framework and Fluoride Anion. Parts a,c and b,d of Figure 4 are respectively projections of the structures reported by Koningsveld et al.[3] and from this study. They clearly show different Si−O−Si distortion of the framework around O15, O9 (Table 5). In the study of Koningsveld et al.[3] the crystal used was synthesized in hydroxide medium (without fluoride) and the OH^- counteranion was not located. This may explain the differences with our results.

In our study, we found a disordered fluoride anion, which breaks the mirror symmetry: the distance between the two Fx mirror images is 0.985(4) Å. At the end of the refinement the occupancy of the fluorine is 0.477(6) (<0.5), preventing unphysical short Fx−Fx contacts and ensuring quasi total charge compensation of the TPA^+. This result differs from other reported results (X-ray powder data of Mentzen et al.[7] and NMR experiments of Fyfe et al.[4]), which locate the F^- anion on the mirror plane inside the $[4^15^26^2]$ cage. These latter two studies had imposed the framework of the structure published by Koningsveld et al.[3] and this may explain part of the discrepancies with our results. It is also important to mention that

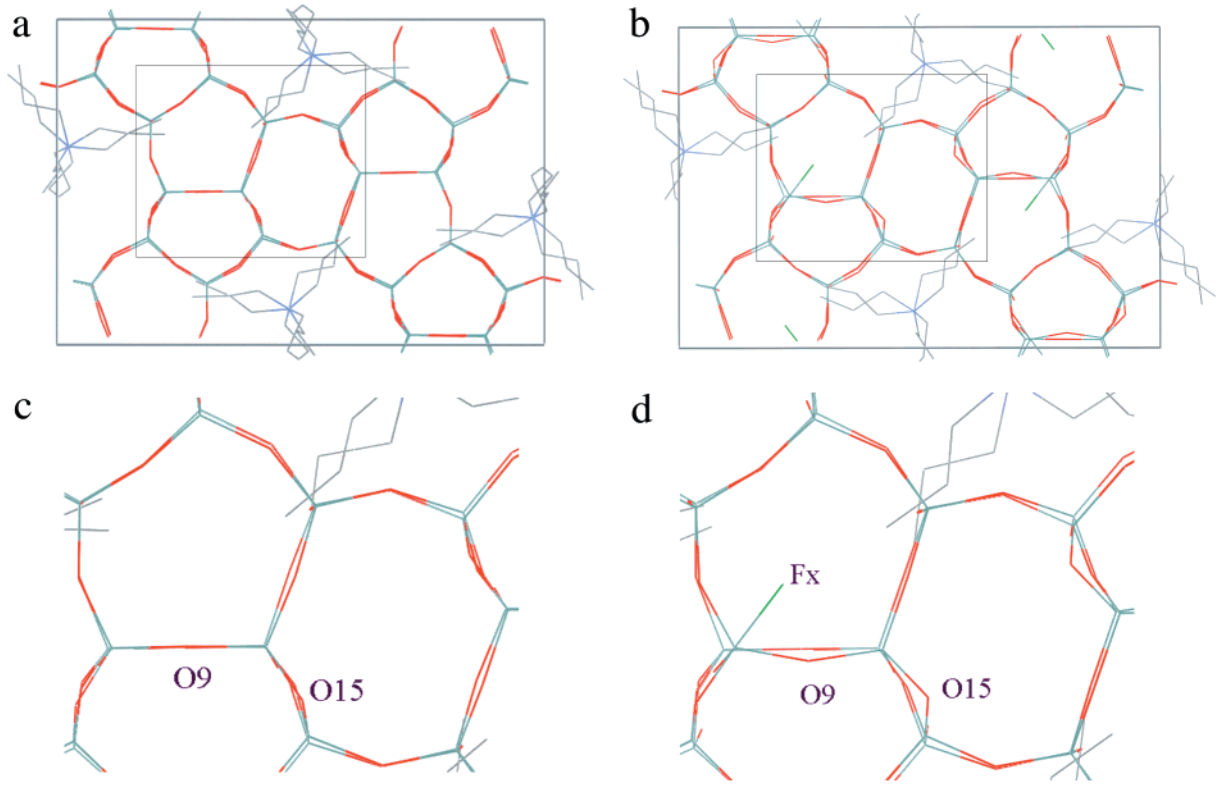

Figure 4. Projections along the [010] direction of (a, c) the structure from Koningsveld et al.[3] and (b, d) the structure from this study. Mirror images of the cations are not shown.

experimental conditions are not exactly the same. First, the compositions of the synthesis gel are different, which may affect the crystal quality.[20] Second, Fyfe et al.,[4] although giving fractional coordinates of the fluoride anion on *m*, report that in fact F^- "is covalently bonded to Si9 in the $[4^15^26^2]$ cage (...) and exchanges between two "mirror-related" Si9 sites, making them equivalent on the NMR time scale". The Si−F distances determined spectroscopically by Fyfe et al. (CP, REDOR, TEDOR) compares with those found in this study. Furthermore, in the study of Fyfe et al., the experiments were done at 327 K, where the spectra are best resolved. This point may be important because several studies evidenced a dynamic behavior of the fluoride anion depending on the temperature (Koller et al.[9,10]).

In our case, the distortion of the framework around the Si9 atom is due to the interaction with the fluoride ion inside the $[4^15^26^2]$ cage. The large Si9 ADP ellipsoid has its major axis almost oriented toward Fx with the mean square displacement along Si9−Fx (0.036 $Å^2$) close to largest ADP ellipsoid principal axis (0.039, 0.009, 0.012 $Å^2$) (Figure 3b), which may indicate a disorder of this silicon atom having, on average, half a fluoride anion in his first coordination sphere (for comparison, the other silicon atoms are more isotropic; see Table 1S). It is also interesting to note that the silicon atoms that exhibit the highest equivalent ADP excluding Si9 are Si6, Si10, and Si8 [0.0159(2), 0.0149(2), and 0.0134(2) $Å^2$ respectively]. These latter atoms are linked to Si9 through, respectively, O18, O9, and O8. This may be related to the disorder induced by Fx on Si9 that propagates through the Si,O framework. The framework oxygen atoms have very spread equivalent ADP ranging from 0.0173(7) $Å^2$ for O25 to 0.0482(9) $Å^2$ for O13. Moreover, these atoms have very anisotropic ADP, indicating a dynamic deviation from the *Pnma* symmetry according to Koningsveld et al..[3]

The existence of $SiO_{4/2}F^-$ units in as-made pure silica crystalline microporous materials synthesized in fluoride media have also been reported for example in the case of ITQ-4 (IFR), nonasil (NON), SSZ-23 (STT), ZSM-12 (MTW), ITQ-3 (ITE), and Beta (*BEA) [24−30]:

Barrett et al.[24] reported XRD structural studies on ITQ-4 zeolite and located F^- inside a $[4^35^26]$ cage, at 2.21(2) Å from a framework silicon atom [and at 2.13(2) Å from an oxygen atom], near a 4MR. However, they found "no NMR evidence for such [Si−F] bonds in ITQ-4".

Structural investigations on single crystals of nonasil (Van de Goor et al.[25]), ITQ-4 (Bull et al.,[26] CCLRC synchrotron, Daresbury) and silicalite (this work) clearly show that silicon atoms can form trigonal bipyramidal $SiO_{4/2}F^-$ units with Si−F distances of, respectively, 1.836(6), 1.913(10), and 1.915(3) Å. It should be noted that in all three of these structures the fluorine atoms have a partial occupancy of about 50%, which implies biased Si−F distances. The geometry of the Si coordination polyhedra are also very similar, with Si−O (apical) longer (∼1.66 Å) than Si−O (basal) (∼1.61 Å).

For the other structures in which F^- was located (octadecasil, Caullet et al.;[27] SSZ-23, Camblor et al.[28]) these geometric characteristics do not clearly show up, but pentacoordinated silicon atoms are reported.[29,10] $SiO_{4/2}F^-$ units were also indicated (but F^- was not located) using NMR techniques in ZSM-12, ITQ-3, and Beta.[10]

For these types of materials (nonasil, ITQ-4, silicalite, ...), one should also note that, as previously reported, for example, by Barrett et al.,[30] fluoride anions are often located near four-membered ring windows (4MR). One can add that for nonasil, ITQ-4, and silicalite, the fluoride anions are even linked to silicon atoms from the 4MR. In pure silica as-made crystalline microporous materials synthesized in fluoride media, penta-coordinated silicon atoms seem to be a rule, not an exception.

TPA Cations. As shown in Figure 4, our results are qualitatively similar to those of Koningsveld et al.[3]: the TPA^+ cations are located at the channel intersections, with their arms C7a−C8a−C9a and C7b−C8b−C9b pointing to straight chan-

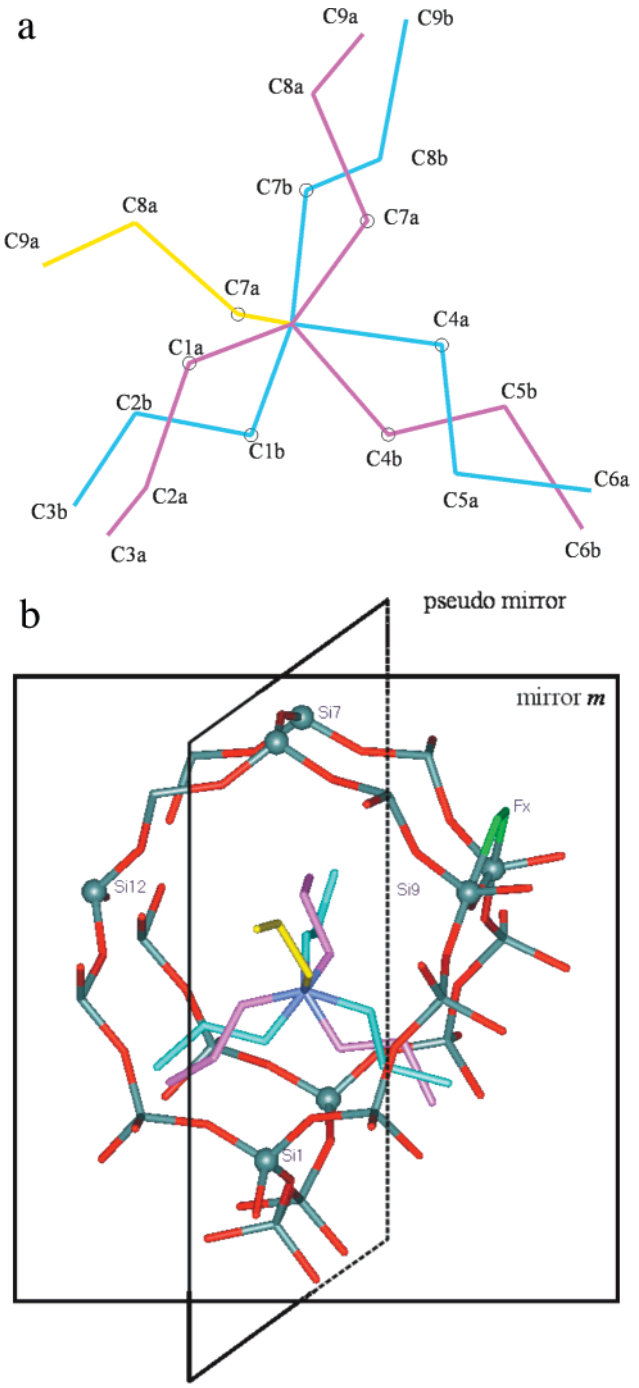

Figure 5. (a) View of the disordered TPA and TPA′ cations. (b) Positions of TPA and TPA′ at the channel intersection; Note that Fx close to Si9 breaks the pseudomirror symmetry. TPA in violet; TPA′ in cyan; the propyl arm common to the two cations in yellow. Mirror images of the cations are not shown.

nels and C1a−C2a−C3a, C4a−C5a−C6a, C1b−C2b−C3b, and C4b−C5b−C6b into sinusoidal channels.

Table 4 lists C−N−C−C torsion angles. In this study torsion angles are close to those proposed by Koningsveld et al.,[3] contrary to those (0°) reported by Baerlocher[6] and Price et al.[5]

The shortest contacts between two possible adjacent TPA^+ are C3b−C6a 3.57(3) Å inside a sinusoidal channel and C9a−C9b 3.71(2) Å inside a straight channel. TPA has also contacts with oxygen atoms of the framework as short as 3.28(2) Å C2a−O1, 3.51(1) Å C9a−O22, 3.52(2) Å C8a−O22, ... These distances should be compared to the sum of van der Waals radii of oxygen and carbon atoms[31] (1.50 + 1.70 = 3.2 Å). It has also to be noted that there are "short" Si−C distances: C9b−Si8 3.91(2) Å and C2a−Si2 3.95(2) Å, which are slightly greater than the sum of their van der Waals radii (2.10 + 1.70 = 3.8 Å).

Koningsveld et al.[3] modeled the TPA^+ cations by defining two orientations of the ammonium, populated in the ratio 3:2, and almost related by a pseudomirror passing through Si1, N, and Si7, which implies similar chemical environments for the two orientations. In our case, TPA and TPA′ do not respect the pseudomirror symmetry (N is at 0.240(5) Å from the plane passing through Si1 and Si7). This pseudosymmetry of the framework is broken between Si9 and Si12 because Si9 is coordinated $SiO_{4/2}F^-$, while Si12 is coordinated $SiO_{4/2}$ (Figure 5b). These differences then may induce peculiar interactions between Si9 and the ammonium.

Conclusion

This study reports the accurate location of the fluoride counteranion in as-synthesized silicalite using single crystal X-ray diffraction at room temperature. This anion lies in the $[4^15^26^2]$ cage and is strongly coordinated with the Si9 framework atom. The latter is therefore pentacoordinated by four oxygen framework atoms and one fluoride anion. This trigonal bipyramid is also present in other pure silica crystalline materials (nonasil,[21] ITQ-4[22]), where it presents similar geometric characteristics. The disordered TPA^+ cations are qualitatively in the same locations found by Koningsveld et al.[3] for hydroxide as-synthesized ZSM-5.

The nature of the disorder may be probed by temperature dependent single crystal X-ray diffraction experiments, but in the case of as-synthesized silicalite-1 a broad phase transition occurs at approximately 175 K[32] and therefore complicates accurate experiments below 175 K.

The localization of fluoride anion close to 4MR may be related to its role as a templating agent contributing to the stabilization of the structure[33] (possibly by enhancing the formation of 4MR entities), in addition to that of mineralizing agent. The arrangement of the TPA arms at the channels intersection, one arm pointing in each channel, also suggests its possible role as a template although all the stabilizing interactions with the framework (in peculiar H bonds) cannot be derived from the disordered averaged X-ray structure.

It should also be noted that the structure derived from this study is that of a crystal after the end of the crystallization process. Linking this results with the "structure" of moieties involved in the gel chemistry is a task going beyond the purpose of this paper.

Acknowledgment. We greatly acknowledge Dr. J. Patarin, Head of the "Laboratoire de Matériaux Minéraux", CNRS UPRES-A 7016, Mulhouse, France, for fruitful discussions. We are grateful to Prof. R. H. Blessing for his helpful remarks and discussions and to Prof. C. A. Fyfe for a copy of ref 4 prior to publication. We thank J. P. Dècle, J. Reymann, and C. Palin for their technical help. The referees are gratefully acknowledged for their constructive suggestions. Structural representations are done with WebLabViewer from Molecular Simulations Inc. After submission of this paper, a similar work on location of extraframework species in Fe/Ga Silicalite-1 (Poster S6.M5.P1, M. Milanesio, D. Viterbo, C. Lamberti, F. Testa, and R. Aiello) was shown at the 20th European Crystallographic Meeting (August 25−31, 2001, Kraków).

Supporting Information Available: Anisotropic atomic displacement parameters for all non-carbon atoms. This material is available free of charge via the Internet at http://pubs.acs.org.

References and Notes

(1) Olson, D. H.; Kokotailo, G. T.; Lawton, S. L.; Meier, W. M. *J. Phys. Chem.* **1981**, *85*, 2238.

(2) Wu, E. L.; Lawton, S. L.; Olson, D. H.; Rohrman, A. C.; Kokotailo, G. T. *J. Phys. Chem.* **1979**, *83*, 2777.

(3) Koningsveld, H. van; van Bekkum, H.; Jansen, J. C. *Acta Crystallogr.* **1987**, *B43*, 127.

(4) Fyfe, C. A.; Brouwer, D. H.; Lewis, A. R.; Chézeau, J. M. Submitted and private communication.

(5) Price, G. D.; Pluth, J. J.; Smith, J. V.; Bennett, J. M.; Patton, R. L. *J. Am. Chem. Soc.* **1982**, *104*, 5971.

(6) Baerlocher, C. *Proceedings 6th International Zeolite Conference*; Butterworth: London, 1984; p 823.

(7) Mentzen, B. F.; Sacerdote-Peronnet, M.; Guth, J. L.; Kessler, H. *C. R. Acad. Sci. Paris* **1991**, t. 313, Série II, 177.

(8) [n^m...] indicates a cage consisting of *m* windows having n silicon atoms (*n* membered ring (MR) windows).

(9) Koller, H.; Wölker, A.; Eckert, H.; Panz, C.; Behrens, P. *Angw. Chem., Int. Ed. Engl.* **1997**, *36*, 2823.

(10) Koller, H.; Wölker, A.; Villaescusa, L. A.; Díaz-Cabañas, M. J.; Valencia, S.; Camblor M. A. *J. Am. Chem. Soc.* **1999**, *121*, 3368.

(11) Porcher, F.; Souhassou, M.; Dusausoy, Y.; Lecomte, C. *C. R. Acad. Sci. Paris* **1998**, t.1, Série IIc, 701.

(12) Porcher, F.; Souhassou, M.; Dusausoy, Y.; Lecomte, C. *Eur. J. Mineral.* **1999**, *11*, 333.

(13) Porcher, F.; Souhassou, M.; Graafsma, H.; Puig-Molina, A.; Dusausoy, Y.; Lecomte, C. *Acta Crystallogr.* **2000**, *B56*, 766.

(14) Guth, J. L.; Kessler H.; Wey R. In *Studies in Surface Science and Catalysis*; Elsevier: Amsterdam, 1986; Vol. 28, p 121.

(15) Weidenthaler, C.; Fischer, R. X.; Shannon, R. D. *J. Phys. Chem.* **1994**, *98*, 12687.

(16) Otwinowski, Z.; Minor, W.; Raynor, J.; Henderson, K.; Majewski, W.; Mohanty, N.; Cymborowski, M. HKL2000, 2000.

(17) Blessing, R. H.; Guo, D. Y.; Langs, D. A. *Intensity statistics and normalization In Direct methods for solving macromolecular structures*; Fortier, S., Ed.; Dordrecht, The Netherlands, 1998; pp 47−71 (and references therein).

(18) Petříček, V.; Dušek, M. The crystallographic computing system JANA2000, 2000, Institute of Physics, Praha, Czech Republic.

(19) *International Tables of Crystallography*; Kluwer Academic Publishers: Dordrecht, The Netherlands; Vol. C.

(20) Chézeau, J. M.; Delmotte, L.; Guth, J. L. *Zeolites* **1991**, *11*, 598.

(21) Chézeau, J. M.; Delmotte, L.; Guth, J. L.; Soulard, M. *Zeolites* **1989**, *9*, 78.

(22) Gougeon, R.; Chézeau, J. M.; Meurer, B. *Solid State Nucl. Magn. Reson.* **1995**, *4*, 281.

(23) Gougeon, R.; Delmotte, L.; Reinheimer, P.; Meurer, B.; Chézeau, J. M. *Magn. Reson. Chem.* **1998**, *36*, 415.

(24) Barrett, P. A.; Camblor, M. A.; Corma, A.; Jones, R. H.; Villaescusa, L. A. *J. Phys. Chem. B* **1998**, *102*, 4147.

(25) Van de Goor, G.; Freyhardt, C. C.; Behrens, P. *Z. Anorg. Allg. Chem.* **1995**, *621*, 311.

(26) Bull, I.; Villaescusa, L. A.; Teat, S. J.; Camblor, M. A.; Wright, P. A.; Lightfoot, P.; Morris, R. E. *J. Am. Chem. Soc.* **2000**, *122*, 7128.

(27) Caullet, P.; Guth, J. L.; Hazm, J.; Lamblin, J. M. *Eur. J. Solid. State Inorg. Chem.* **1991**, *28*, 345.

(28) Camblor, M. A.; Díaz-Cabañas, M. P.; Perez-Pariente, J.; Teat, S. J.; Clegg, W.; Shannon, I. J.; Lightfoot, P.; Wright, P. A.; Morris, R. E. *Angew. Chem., Int. Ed. Engl.* **1998**, *37*, 2122.

(29) Fyfe, C. A.; Lewis, A. R.; Chézeau, J. M.; Grondey, H. *J. Am. Chem. Soc.* **1997**, *119*, 12210.

(30) Barrett, P. A.; Boix, E. T.; Camblor, M. A.; Corma, A.; Díaz-Cabañas; M. J.; Valencia, S.; Villaescusa, L. A. *12th International Zeolite Conference*; Treacy, M. M. J., Marcus, B. K., Bisher, M. E., Higgins, J. B., Eds.; Materials Research Society: Warrendale, PA, 1999; p 1495.

(31) Bondi, A. *J. Phys. Chem.* **1964**, *68*, 441.

(32) Chézeau, J. M.; Delmotte, L.; Hasebe, T.; Chanh, N. B. *Zeolites* **1991**, *11*, 729.

(33) Guth, J. L.; Kessler, H.; Caullet, P.; Hazm, J.; Merrouche, A.; Patarin, J. In *Proceedings from the Ninth International Zeolite Conference*; von Ballmoos, R., Higgins, J. B., Treacy, M. M. J., Eds.; Butterworth-Heinemann: Boston, MA, 1992; Vol. I, p 215.

(34) Johnson, C. K. *Report ORNL-5138*; Oak Ridge National Laboratory: Oak Ridge, TN, 1976, ORTEP II.